Submitted to Journal of Physics and
Chemistry of Solids

LBL-119 Rev.
Preprint c.1

STABILITY OF A15 TYPE PHASES

L. D. Hartsough

August, 1974

Prepared for the U. S. Atomic Energy Commission
under Contract W-7405-ENG-48

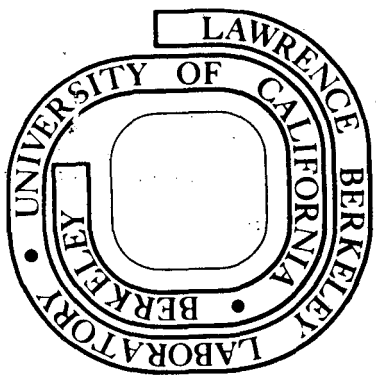

LBL-119 Rev.
c.1

DISCLAIMER

STABILITY OF A15 TYPE PHASES

L. D. Hartsough*

Inorganic Materials Research Division, Lawrence Berkeley Laboratory and Department of Materials Science and Engineering, College of Engineering; University of California, Berkeley, California

Previous works dealing with the stability of the A15 phases are reviewed. Data for over 60 known A15 phases are used to develop criteria for stability which may be applied to hypothetical A15 phases. Occurrence of these phases is examined in terms of the valence bond concepts of the Engel-Brewer correlation and in its frequency with changes in electronic density of states. A15 is most favored when the "A" elements are V, Nb, or Cr, when radii of the constituent atoms differ by no more than 8%, at compositions determined by electron concentration, and at relatively low temperatures. Composition and temperature of formation are predicted for several likely hypothetical A15 phases.

*Present address: Optical Coating Laboratory, Inc., P. O. Box 1599, Santa Rosa, California 95403

INTRODUCTION

Intermetallic compounds with the A15 (cubic Cr_3Si-type) structure have been found to exhibit high values of superconducting critical temperature, magnetic field, and current carrying capacity (1). Consequently, much effort has been expended in efforts to understand the stability of A15 phases and to discover new ones. Many new A15 phases have been found in recent years, but most of the exploration was guided by relative atomic size and position of the components in the Periodic Table. Recognition that A15 phases are electron phases is relatively recent (2), although Brewer (3) promoted this concept as early as 1964. Thus, the 3:1 atomic composition ratio indicated by the usual chemical notation for these phases (A_3B) is not rigorously followed, especially where both components are transition metals. Despite this recognition, A15 is yet to be found in a number of binary systems for which it seems favorable.

This paper will re-examine the operation of parameters mentioned above, as well as several others, and present guidelines which can be used to determine systems, compositions, and temperatures favorable to formation of new A15 phases. First, parameters to be examined will be introduced. Then, previous work will be reviewed to provide an historical perspective. Next, the criteria will be developed and summarized. Finally, several binary systems which are favorable for formation of new A15 phases will be mentioned.

FACTORS TO BE EXAMINED

Factors correlated with stability of metallic phases may be categorized as geometrical, electrochemical, and thermodynamic (4,5). Of the geometrical factors, relative atomic size is easiest to compute and has long been recognized as important in determining extent of primary solid solution (4) and occurrence of the Laves phases (6). Other geometrical factors (4,7) (usually invoked in examination of relative stability of specific competing phases at one composition)

are beyond the scope of this paper.

The electrochemical factors may be approached from a physical or a chemical point of view. From the former, electron concentration (number of electrons per atom, per unit cell, or per unit volume) is related to electron energy band structure and to density of states at the Fermi surface, N(O). The chemical viewpoint relates electron concentration to filling of bonding orbitals by electron transfer or promotion from nonbonding to bonding valence states. From either viewpoint there are certain types of phases in which electron concentration plays a major role in stability. These are called electron compounds, or more properly, electron phases.

Thermodynamic parameters to be discussed are temperature and pressure. In addition to these, internal pressure will be mentioned as a secondary factor in discussion of the Engel-Brewer correlation. Internal pressure is the term used by Brewer (3) for the solubility parameter or "cohesive energy density" term in regular solution theory (8). It is the molal energy of vaporization divided by the molal volume and is a measure of internal cohesive forces. Internal pressure differences are used to calculate the non-electronic contribution to excess thermodynamic functions of mixing and solubility limits of solutions (3,8,9).

HISTORICAL PERSPECTIVE

Beta-tungsten was discovered in 1931 as (perhaps unfortunately) the prototype of the structure now designated A15 (Strukturbericht) or Cr_3Si-type. Whereas in β-W the lattice sites are all occupied by one species, constituents of binary A15 phases prefer one or the other of the types of sites shown in Fig. 1. See Pearson (10) for details concerning the A15 lattice. Kasper (11) pointed out certain geometrical similarities among the α-Mn (or χ), σ, A15, μ, and Laves phases. For σ and A15, structurally quite similar,

a particular species of atom has the same coordination in each. Both structures have chains of atoms along which the interatomic spacing is about 15% shorter than in the pure element (12). This has been interpreted (13,14) to mean that covalent bonding is strong along the chains. It was also suggested (15) that the contraction in A15 phases is related to geometrical packing principles and that stability depends on the constituent atoms' ability to undergo large deformation. Laves (13) observed that a radius ratio (Goldschmidt CN 12) near one seems to be favored and called attention to regularities in position of the constituents in the Periodic Table: the A element is always to the left of the Mn Group and the B element always in or to the right of the Group.

In the late 1950's and early 1960's a number of non-stoichiometric A15 phases containing transition metals as the B element were discovered. Waterstrat and Van Reuth (2) showed that the composition shift with increasing Group number was similar to that in σ phases and suggested that similar factors affect stability. For σ phases formed from Groups 6-8 3d elements, it was shown (16-18) that number of electron vacancies in the 3d shell correlated with composition limits better than did total number of electrons per atom outside a closed shell. However, difficulties arose in determining number of electron vacancies for early 3d, 4d, and 5d metals (19). The electron vacancy concept is equivalent to saying that the extent of d shell filling determines phase boundaries.

In contrast, the Engel correlation (20) assumes that it is the number of bonding s,p electrons which correlates with crystal structure. This concept, akin to Pauling's valence bond approach (21), was refined and used by Brewer (3,22,23,24) to predict phase boundaries in many intertransition metal systems. The procedure is to find the distribution between d and s,p electrons which results in highest net bond energy, given values for the contribution from each type of bond and

the energy paid to achieve this distribution. (Although Pauling electronegativity difference is the traditional measure of tendency to transfer electrons, it is unsatisfactory for calculations of electronic interactions in intertransition metal systems (9,25) where d electrons participate in bonding.) Then, subject to limitations placed on size, internal pressure differences, and degree of electron transfer, the number of s,p electrons determines structure. The order in which such electron phases appear as s,p electron concentration increases is bcc, A15, σ, μ, χ (3). Thus, the phases in competition with A15 will typically be the bcc terminal solid solution and the σ phase. The s,p electron concentrations (electrons per atom) over which these phases occur are (26):

e/a	phase
1.0 - 1.5	bcc
1.1 - 1.7	A15
1.2 - 1.9	σ

Because of considerable overlap in electron concentration ranges, the other factors mentioned above must be considered when comparing stability of the A15 phase to that of competing phases.

Brewer (3,26) discussed several of the factors important in understanding stability of A15 relative to bcc and σ in intertransition metal systems. In A15, distortion of the A atom, perhaps for sterichemical reasons, allows better d bonding than occurs in bcc. This is especially true in the first long Period; in the third long Period (5d metals) d orbitals are stongly bonding in the bcc phase and little is gained by distortion. To arrive at the electron concentration range for A15 stability, Brewer assumed that the A metal achieves a d^5 configuration. However, this may be true only for the Cr-Group and for V and Nb, which seem to utilize extra d-bonding most effectively (23). The configuration for Ti and Zr is probably fewer than five d electrons. The later 5d elements are favored as B components in A15 because of

their size and d bonding ability. According to Brewer, A15 will be favored where internal pressure difference limits bcc to less than its maximum e/a ratio.

Crystallographic order is an important factor in the high temperature stability of phases, because of its effect on entropy. It can also indicate types of bonding. Order is the extent to which a particular type of site is filled by one species of atom. The usual Bragg-Williams order parameter is defined as $S_a=(r_a-F_a)/(1-F_a)$, where r_a is the fraction of A sites occupied by a-atoms and F_a is the fraction of a-atoms in the phase. Waterstrat and Van Reuth (15) discuss its meaning for non-stoichiometric A15 phases, which are usually as ordered as composition will allow. More disorder is found in bcc solid solutions and σ phases. The latter have five types of lattice sites and occur over a wide combination of elements and range of compositions (3,27), yet maintain the correct electron concentration. Disorder does not seem to destabilize A15 when its constituents are from Groups close to one another (15), as shown by existence of the A15 phases $Mo_{45}Tc_{55}$, $V_{48}Os_{52}$, and $V_{63}Ir_{37}$.

Careful studies of order (15), composition (28), and superconductivity (29) in such A15 phases led Waterstrat and co-workers to postulate relationships between bonding, order, and band structure. It was found (28) that order in $Cr_{72}Os_{28}$ was not as high as theoretically possible and was insensitive to temperature. They suggested that the mixture of atoms on each type of site is controlled by the extent of d-electron overlap. Elements closest to the Mn-Group would have the most d-orbitals available for bonding, allowing increased complexity in overlap and more mixing of the atoms. The Labbe-Friedel band structure model for A15 phases (30,31) was used in explaining this idea. In this model there are three sharp peaks in the density of states, representing three bonding sub-bands of the d band.

These three sub-bands are not clearly evident in the density of states curve for V_3Ga calculated by Mattheiss (32). His band structure calculations are supported by x-ray emission spectra of Cr_3Si (33) and V_3Si (34). Figure 2 shows density of states vs electrons per atom for A15 (V_3Ga) and bcc (Nb) computed from values given by Mattheiss (32,35). The lower peak for the A15 density of states (36-39 electrons/unit cell) is for phases in which the B element is a non-transition metal and the upper (44-56 electrons/cell) is for those with a transition metal as B component. Calculations of the charge distributions (32) indicated that the atoms in V_3Ga are about neutral, but with considerable admixture of gallium s and p and vanadium d wave functions. With V_3Co strong interactions between overlapping d bands were found. Thus, the energy band structures for these types of A15 phases are considerably different. The limited mutual solubilities of the two types might be due to this. Nevitt (36) has interpreted the immiscibility as an indication that different kinds of bonding exist.

The nature of bonding in metallic transition-nontransition metal phases is a controversial subject (37). Brewer (23) interpreted trends in atomization energies to indicate that B,C,N, and Si contribute electrons to the transition metal, allowing it to achieve an electronic configuration of optimum bonding strength. Pauling (21) discussed electron transfer between "hyperelectronic" and "hypoelectronic" metals. The former occur to the right of the Copper Group and the latter to the left of the Vanadium Group. Unusually short bond lengths in intermetallic phases of these two groups were taken to indicate electron transfer from hyperelectronic to hypoelectronic element. Since this is opposite to the direction of charge transfer predicted from electronegativity difference, the extra stability indicated by shortened bond lengths was accounted for by the electroneutrality principle. The views presented above are supported by some band structure calculations for TiC (38,39), but are contradicted by other calculations (40) and experimental results (41,42). Because of the uncertainties

concerning bonding in these systems, it is perhaps best to depend upon empirical correlations for predictions of A15 phase occurrence.

DEVELOPMENT OF CRITERIA

Binary systems in which A15 phases have been reported (prior to December 1971) are shown in Fig. 3, where B elements are shown as they appear in the Periodic Table. Each B position is divided into 9 sub-cells, one for each of the elements which occupy A sites in the A15 lattice. (Because no A15 phases containing Hf have been reported, each B component is identified in its lower left sub-cell). Where data are from readily available sources (27,43-47) an "X" is entered in the appropriate sub-cell. If A15 has been reported subsequent to the compilations, a reference number is given. Phases which, in the author's opinion, need to be confirmed are denoted with a "?". Some ambiguity surrounds other phases not listed in Fig. 3. Cr_3O(45) was reported but not confirmed (29). It was suggested that Mo_3Zr was probably oxygen stabilized (44). Uranium hydrides listed by Laves (13) as A15 were given by Hansen and Anderko (44) as simple cubic and primitive cubic (32 atoms per unit cell). Pearson (43) apparently does not accept the A15 structure for these U phases. The phases Nb_3In, Nb_3Bi, and Mo_3Sn are stabilized by high pressure; the latter two have been formed solely in this way. From Fig. 3 it can be seen that Laves' observation (13) about the positions of the A and B elements in the Periodic Table is still valid.

The bar chart in Fig. 4 shows the number of confirmed A15 phases occurring within 0.04 wide ranges of R_A/R_B (Goldschmidt CN12). A radius ratio slightly less than one seems to be favored: the average value is 0.987. There are 26 phases which occur between 0.92 and 1.00, while 22 are in the range 1.00 to 1.08. Together, these account for 80% of the A15 phases. Thus, A15 is favored when the B radius is within 8% of the A radius.

We now examine lattice parameter trends for evidence of bonding type. The data are shown in Fig. 5, an updated version of one of Nevitt's figures (27), where a_o is plotted against the CN12 radius of B. Radii of the A components are given by arrows on the abscissa. It can easily be seen why the existence of several reported phases was questioned, especially for V with In, Ti, Pb, and Bi. Several observations can be made from this figure. First, the assertion (28,56,57) that Gold should be treated as a transition metal is in each case born out by lattice parameter trends. Second, the lattice contraction is greater when B is a non-transition element, perhaps indicative of a larger ionic contribution to bonding. Third, in several instances Hg and Sn have size effects consistent with transition metals, especially with Ti and Zr. Fourth, the larger B elements have proportionately less effect on a_o than do the others. This may be a bonding effect, or it may indicate that an upper limit to the A-A distance is being approached. However, there is also a composition effect in these phases, most of which deviate from the ideal 3:1 atomic ratio. Prediction of A15 lattice parameter will be covered in a separate paper.

Composition ranges reported for A15 phases are given in Figs. 6a-g*, with lines of constant electron concentration sketched in for reference. In some cases phase boundaries were not determined in detail, in several others the authors assumed the phase to occur at the ideal composition. In spite of these uncertainties, there are instances where phase boundaries show an electron concentration effect. This has previously been observed and commented upon for systems where B is a transition metal, as reviewed in the previous section. However, in many cases B-rich boundaries in non-transition metal systems also follow electron concentration. This is rather surprising for the following reasons. In the valence bond approach, stability of A15 arises from extra d-bonding, presumably largely along A-A chains, made available by atomic arrangements in the structure.

*In addition, the A15 phase was detected (54) in W alloys containing 13-45% Re. These were formed by decomposition of the hexafluorides at 500°C. No analysis for oxygen impurity was

Any substitution of non-transition metals in these chains would decrease d-bonding and destabilize the structure. Thus, B-rich boundaries would be controlled by the disorder imposed by off-stoichiometric composition, while A-rich boundaries would follow electron concentration. The figures show the opposite tendency, although the latter boundaries follow electron concentration in some transition metal systems. The B-rich boundaries shown usually exist at high temperature, where entropy of A-B mixing may serve to counteract the destabilization effect discussed above.

The role of vacancies in off-stoichmetric A15 phases should be discussed. Evidence suggests (2,15,29) that in transition metal A15 phases deviations from stoichiometry are accommodated by atomic substitution. Where the B element is not a transition metal, excess A usually goes into B sites (58-61), but a defect structure is possible (62) in heat treated samples. In this case A atoms migrate to B sites, made available by volatilization, leaving vacancies on A sites. A few nontransition A15 phases - Nb_3Al, V_3Ga, and Cr_3Si - can have more than 25 at. % B element. The available evidence (61) suggests that excess B goes into A sites. Thus, no vacancies were assumed in calculations of electron concentration used here.

Another effect is shown by the replotted data in Figs. 72a-i. The B elements chosen are those which form the most A15 phases. It takes less B to stabilize A15 as A elements within a Group go from 3d to 5d. Sometimes both A- and B-rich boundaries follow this trend, although the latter do so most strongly. According to the Engle-Brewer approach, 3d bcc metals have substantially less strength per d bond than do 5d. Thus, the former have relatively more electrons promoted to s,p orbitals. The above data are consistent with Brewer's contention (3) that d-bonding strength is markedly increased for 3d metals in the A15 phase. To make up for the resultant depletion of s,p orbitals, more B element (i.e., s,p electrons) must be added. Of course, the composition shifts shown here could be due to

band structure effects. However, knowledge of differences in band structure among A15 phases is still too sketchy to look for such subtle effects. The gross correlation between band structure and occurrence of A15 phases is discussed next.

The range in e/a (total electrons/atom outside a closed shell) over which bcc occurs is about 3.5 to 6.5, while A15 occurs from about 4.0 to 7.0. As can be seen from Fig. 2, both structures have two nearly coincident peaks in N(E) at 4.75 and 6.76 e/a. Thus, if stability is related to these peaks, judgement about relative stability of bcc and A15 is difficult. The band structure of σ phases has not been calculated, although they occur in the range 5.6 to 7.7 e/a (5).

There is a strong correlation between occurrence of A15 and density of states, as shown in Fig. 8. It appears that A15 is favored at compositions which maximize N(O). The grid used in the histogram corresponds to an increase of one in e/a of B (at 3:1 ratio of A:B). If ternary data were included, a narrower grid would be more appropriate. Phases which occur below 32 electrons/cell are Ti and Zr with Hg and Tl. This could be due to a lower d electron concentration achieved by Ti and Zr than for other A elements, as postulated by Brewer. Another possibility is that, with Ti and Zr, the d electrons in Hg and Tl participate in bonding, resulting in a higher electron concentration than calculated here. In general, however, one can treat Fig. 8 as representing probability of occurrence of A15 as a function of electron concentration, with maxima at 4.7 and 6.4 e/a.

Thermodynamic factors will now be examined. Only a short discussion of pressure is required*. For transition metals decreasing the interatomic distance favors phases which can utilize the maximum number of bonding d electrons (64), because d orbitals begin to overlap. Hence, for 3d and 4d

---

*For a more extended discussion see (63).

metals of Groups 4-6 pressure will stabilize A15 over bcc.

Stability of competing phases as temperature increases is determined by the balance between enthalpy and entropy. Structures with high entropy, such as bcc and σ, are favored over A15 at high temperatures. However, A15 phases with the highest bond strength (enthalpy) - those with 3d and 4d transition metals - are stable enough to melt congruently.

Readily available phase diagram information was used to classify 40 A15 phases according to type of reaction by which they form and/or temperature to which they are stable. A Formation Temperature Ratio (FTR) was used to enable comparison with competing phases. FTR is defined as the maximum (absolute) temperature at which A15 is stable divided by the weighted mean of the maximum temperatures for the competing solid phases. Figure 9 illustrates calculation of FTR for the case where A15 forms peritectically and the competing phases melt congruently. Figure 10 presents the data and shows a fairly even representation over the Periodic Table, except for Group 6 non-transition elements. The data are summarized in Table I. A further classification reveals that over half of these A15 phases form by a solid state reaction. It must be emphasized that these results, especially relative frequencies of reaction types, do not hold for the total population of A15 phases. In the author's view more data will reveal that the average FTR is lower than its present 0.80 and that a higher proportion of A15 phases form by solid state reaction. In fact, many recently discovered A15 phases were found by such relatively low temperature techniques as solid state diffusion (49), low temperature annealing of alloys (48), high pressure (66,67) and condensation of the vapors (51,52,54). Because of inadequate data many such phases were not included in the above calculations.

SUMMARY OF CRITERIA

Each of the factors - geometrical, electrochemical, and thermodynamic - plays a role in determining binary systems in which A15 occurs and the composition and temperature at which it is stable. A determination of relative importance among these factors has not been attempted, although some work toward this end has been done (9). The conclusions are presented as a procedure to determine the likelihood of finding A15 for a particular binary system.

First, the A element is a Group 4,5, or 6 transition metal and the B element is from Groups to the right, up to Group 5A. Second, the tendency of A elements to form A15 decreases approximately in the order V, Nb Cr, Ti, Mo, Zr, Ta, W, Hf. Third, the size ratio R_A/R_B (CN12) should be between 0.92 and 1.08. Figure 4 may be taken to express the probability of A15 occurrence as a function of size ratio. Fourth, the most likely composition is strongly affected by electron concentration. Figures 6 and 7 or those of Brewer (3) may be used to determine this composition by extrapolation from known systems. Figure 8 is an expression of the probability of finding A15 as a function of e/a (except perhaps for systems with Ti and Zr) and shows the strong correlation between A15 occurrence and density of states. Fifth, A15 will likely form by a solid state reaction. Finally, the maximum temperature at which it will form is given by an FTR $\leq$ 0.80. FTR is defined in Fig. 9. In many cases, this temperature will be too far below the melting point for any method save vapor deposition to be successful. Each binary system must be considered individually and all known data about its phase diagram should be taken into account.

BINARY SYSTEMS FAVORABLE FOR A15

Perusal of Fig. 3 reveals that there are over 150 binary systems which could be examined in terms of the first criterion.

Here, only a selection from the most probable candidates will be mentioned. The A15 phases predicted by Brewer (3) will not be covered here. References 44-46 should be consulted for phase relationships. All compositions are given in atomic percent.

V-Re A15 should form at about 65% Re, at less than 700°C. Addition of small amounts of Os would decrease the range of bcc (V) and lower the σ eutectoid, favoring peritectoidal formation of A15 from bcc and σ.

Nb-Re A15 is favored to form peritectoidally from χ and bcc (Nb) at the equiatomic composition, since σ exists only at high temperature. The formation temperature is probably below 1200°C.

Mo-Re It has been found (68) that A15 Mo_5Pt dissolves Re to a composition of about $Mo_{67}Re_{24}Pt_9$ at 1600°C and that Re increases the temperature range of stability. However, bcc was found in $Mo_{70}Re_{30}$ at 2000°C. Extrapolation gives A15 near 40% Re. The maximum temperature of formation would be below the σ eutectoid at 1150°C.

Ta-Al The σ phase is compositionally rather wide (20-36% Al) and probably forms peritectically at 2100°C, while bcc (Ta) is limited in composition. Thus, A15 probably forms peritectoidally below 1400°C at a composition between 13 and 18% Al. The existence (69) of a hexagonal oxygen stabilized phase in this region may make it difficult to find A15.

Ta-Ga Ta_5Ga_3 has been reported to have the W_5Si_3 type structure, which is the structure competing with A15 in systems of Mo, V, and Cr with Si and Ge. Cr_5B_3-type has also been reported (70); however, these authors found the W_5Si_3 structure in an alloy with 25% Ga

annealed at 1000°C in a quartz tube. A15 is favored at a composition of about 16% Ga.

W-Ru The σ phase resorbs eutectoidally at 1667°C and 40% Ru, while bcc (W) dissolves about 13% Ru. Thus, A15 is favored from 20-30% Ru and probably forms peritectoidally from (W) and (Ru) below 1500°C.

Zr-Sb The extrapolated composition for A15 is at 17% Sb. A body centered tetragonal phase, Fe_3P-type, has been reported at 25% Sb. The A15 phase probably forms below 600°C.

ACKNOWLEDGEMENTS

This work was done under the auspices of the Atomic Energy Commission. The author wishes to thank Leo Brewer, Victor Zackay, and Robert Hammond for encouragement, advice and helpful discussions.

REFERENCES

1. NEWHOUSE, V.L., In Superconductivity (Edited by R.D. Parks) Vol. 2, pp 1286-1288, Marcel Dekker Inc., New York (1969).

2. WATERSTRAT, R.M., and Van REUTH, E.C., Trans. AIME, 236, 1232 (1966).

3. BREWER, LEO, In High Strength Materials, (Edited by V.F. Zackay) pp 12-103, J. Wiley and Sons, New York (1965).

4. BARRETT, CHARLES and MASSALSKI, T.B., Structure of Metals, Third Edition, Ch. 13, McGraw-Hill, New York (1966).

5. HUME-ROTHERY, WILLIAM, In Phase Stability in Metals and Alloys (Edited by Peter S. Rudman, John Stringer and Robert I. Jaffee) pp 3-24, McGraw-Hill, New York (1967).

6. See Ref. 4, pp 256-259.

7. ALTMANN, S.L., COULSON, C.A. and HUME-ROTHERY, W., Proc. Roy. Soc., A240, 145 (1957).

8. HILDEBRAND, JOEL H., PRAUSNITZ, JOHN M., and SCOTT, ROBERT L., Regular and Related Solutions, Ch. 6, Van Nostrand, Reinhold, New York (1970).

9. KAUFMAN, LARRY and BERNSTEIN, HAROLD, In Phase Diagrams: Materials Science and Technology, Vol. I (Edited by Allen M. Alper) pp. 45-112, Academic Press, New York (1970).

10. PEARSON, W.B., Lattice Spacings and Structures of Metals and Alloys, p. 884, Pergamon Press, Oxford (1958).

11. KASPER, J.S., In Theory of Alloy Phases, pp. 264-278, American Society for Metals, Cleveland (1965).

12. GREENFIELD, P., and BECK, P.A., J. of Metals 8; Trans. AIME 206, 265 (1956).

13. LAVES, F., in Ref. 11, p. 183 ff.

14. MILLNER, T., J. Inorg. Chem. USSR 3, 945 (1958).

15. Van REUTH, E.C., and WATERSTRAT, R.M., Acta Cryst. B24, 186 (1968).

16. DAS, K., RIDEOUT, S.P., and BECK, P.A., Trans. AIME 194, 1071 (1952

17. WOODYATT, L.R., SIMS, C.T., and BEATTIE, JR., H.J., Trans. AIME 236, 519 (1966).

18. MIHALISIN, J.R., BIEBER, C.G. and GRANT, R.T., Trans. AIME 242, 2399 (1968).

19. MURPHY, H.J., SIMS, C.T. and BELTRAN, A.M., J. of Metals AIME 46, (1958)

20. ENGEL, N.N. Some New Viewpoints on the Metallic Bond, Ingenioren, M101 (1939), M1 (1940); Haandlogi Metalare:Selskabet for Metalorskning, Copenhagen, 1945; Kem. Maanedsbled, No. 5,6,8, 9 and 10 (1940), (in Danish). A mimeographed manuscript in English was circulated in this country in the late forties and early fifties. A brief summary is given in Powder Metallurgy Bulletin, 7, 8 (1954).

21. PAULING, LINUS, The Nature of the Chemical Bond, p. 431, Cornell University Press, Ithaca, (1960).

22. BREWER, LEO, Ref. 5, p. 41.

23. BREWER, LEO, in Electronic Structure and Alloy Chemistry of the Transition Metals, (Edited by Paul A. Beck), pp 221-235, Interscience Publishers, New York (1963).

24. BREWER, LEO, Acta Met. 15, 553 (1967).

25. See Ref. 5, pp. 337-341.

26. See Ref. 5, p. 350.

27. NEVITT, M.V., In Ref. 23, pp 101-178.

28. WATERSTRAT, R.M. and van REUTH, E.C., In Ordered Alloys: Structural Applications and Physical Metallurgy (Edited by B. H. Kear, C.T. Sims, N.S. Staloff and J. H. Westbrook), pp 95-110, Claitors Publishing Division, Baton Rouge (1970).

29. BLAUGHER, R.D., HEIN, R.E., COX, J.D. and WATERSTRAT, R.M., J. Low Temp. Physics 1, 539 (1969).

30. LABBE, J. and FRIEDEL, J., J. Phys. Radium 27, 153, 303 (1966).

31. LABBE, J., BARISIC, S. and FRIEDEL, J. Phys. Rev. Letters 19, 1039 (1967).

32. MATHEISS, L.F., Phys. Rev. 138, 112 (1965).

33. NEMNONOV, S.A. and KURMAEV, E.Z., Phys. Stat. Sol. 24, K43 (1967).

34. KURMAEV, E.Z. and NEMNONOV, S.A., Phys. Stat. Sol. (b)43, K49 (1971)

35. MATTHEISS, L.F., Phys. Rev. B 1, 373 (1970).

36. See Ref. 5, p. 347.

37. See Ref. 5, p. 355

38. LYE, R.G., In Atomic and Electronic Structure of Metals, (papers presented at a seminar Oct. 29-30, 1966) pp 99-125, American Society for Metals, Metals Park, Ohio (1967).

39. LYE, R.G. and LOGOTHETIS, E.M., Phys. Rev. 147, 622 (1966).

40. ERN, V. and SWITENDICK, A.C., Phys. Rev. 137, A1927 (1965).

41. RAMQVIST, L., HAMRIN, K., JOHANSSON, G., FAHLMAN, A. and NORDLING, C., J. Phys. Chem. Solids 30, 1835 (1969).

42. RAMQVIST, L., EKSTIG, B., KALLNE, E., NORELAND, E., and MANNE, R., J. Phys. Chem. Solids 30, 1849 (1969).

43. PEARSON W.B., Lattice Spacings and Structures of Metals and Alloys, Vol. 2, Pergamon Press, Oxford (1967)

44. HANSEN, Max and ANDERKO, Kurt, Constitution of Binary Alloys, McGraw-Hill, New York (1965).

45. ELLIOTT, Rodney P., Constitution of Binary Alloys, First Supplement, McGraw-Hill, New York (1965)

46. SHUNK, Francis A., Constitution of Binary Alloys, Second Supplement, McGraw-Hill, New York (1969).

47. MATTHIAS, B.T., GEBALLE, T.H. and COMPTON, V.B., Rev. Mod. Phys. 35, 1 (1963)

48. VIELHABER, E. and LUO, H.L., Solid State Commun. 5, 221 (1967).

49. SAVITSKII, E.M., BARON, V.V. and EFIMOV, Y.V., Soviet Physics-Doklady 11, 988 (1967).

50. HOLLECK, H., NOWOTNY, H., and BENESOVSKY, F., Mh. Chem. 94, 473 (1963).

51. HARTSOUGH, L.D., and HAMMOND, R.H., Sol. State Commun. 9 885 (1971).

52. HANAK, J.J., GITTLEMEN, J.I., PELLICANE, J.P. and BOZOWSKI, S., J. Appl. Phys. 41, 4958 (1970).

53. HOLLAN, L., LECOCQ, P. and MICHEL, A., Compt. Rend. Acad. de Sci., Paris 260, 2233 (1965).

54. FEDERER, J.I. and STEELE, R.M., Nature 205, 587 (1965).

55. RAUB, E. and ROOSCHEL, E., Naturwiss, 53, 17 (1966); Z. Metallk, 57, 470 (1966).

56. MATTHIAS, B.T., J. Phys. Chem. Solids 10, 342 (1959).

57. ROBERTS, B.W., in Intermetallic Compounds (edited by J.H. Westbrook) p. 588, John Wiley and Sons, New York (1967).

58. REED, T.B., GATOS, H.B., LaFLEUR, W.J. and RODDY, J.T., in Metallurgy of Advanced Electronic Materials, Vol. 19 (Edited by G.E. Brock), p. 71, Interscience Publisher, New York (1963).

59. MULLER, A., Z. NATURFORSCH, 25A, 1659 (1970).

60. NEWKIRK, L.R. and TSUEI, C.C., Phys. Stat. Sol. (a) 4, 387 (1971).

61. LEVINSTEIN, H.J., WERNICK, J.H., and CAPIO, C.D., J. Phys. Chem. Solids 26, 1111 (1965).

62. BACHNER, Frank J. and GATOS, Harry C., Trans. AIME 236, 1261 (1966).

63. WENGERT, Paul Richard, Thermodynamic Stability of Certain Intermetallic Compounds Made from Transition Elements (Ph.D. Thesis) UCRL-18727, Appendix A1, Lawrence Berkeley Laboratory, Berkeley (1969).

64. BREWER, L., Science 161, 115 (1968).

65. ZENER, C., in Ref. 5, pp 25-38.

66. BANUS, M.D., REED, T.B., GATOS, H.D., LEVINE, M.C. and KAFALAS, J.A., J. Phys. Chem. Solids 23, 971 (1962).

67. KILPATRICK, D.H., J. Phys. Chem. Solids 25, 1213 (1964).

68. ROSCHEL, E. and RAUB, E., Z. Metallk, 61, 71 (1970).

69. RAMAN, A., Aluminum 41, 318 (1965).

70. HOLLECK, H., RIEGER, W., NOWOTNY, H. and BENESOVSKY, R., Monatsh, Chem. 94, 841 (1963).

TABLE I FORMATION REACTION AND TEMPERATURE RATIO FOR FORTY A15 PHASES

REACTION TYPE	NUMBER OF SYSTEMS	AVERAGE FTR
Congruent melting	6	0.91
Peritectic	11	0.90
Peritectoid	19	0.71
Congruent from Solid	4	0.69

FIGURE CAPTIONS

Fig. 1. The cubic A15 (Cr_3Si-type) structure. The A type sites (shaded) form three orthogonal chains along the cube faces. B type sites are the body centered cubic positions.

Fig. 2. Density of states for bcc Nb and A15 V_3Ga as functions of electron concentration. Constructed from the calculations of Mattheiss (33,36). Above 4 e/a, the peaks and valleys in N(E) are roughly coincident.

Fig. 3. Occurrence of Binary A15 phases in the Periodic Table. See text for explanation.

Fig. 4. Number of confirmed A15 phases as a function of atomic radius ratio (Goldschmidt CN12).

Fig. 5. Lattice parameter of A15 phases vs size of B atom (after Nevitt (27)). For data, see references given for Fig. 3. Vertical arrows on abscissa give sizes of the A atoms.

Fig. 6. (a-g) Composition ranges reported for binary A15 phases formed with a given A element. The curved lines follow constant e/a and are for reference only.

Fig. 7. (a-i) Composition ranges reported for binary A15 phases formed with a given B element. Within a group of A elements (e.g. V, Nb, Ta) less B is required to stabilize A15 as the Period number of the A element increases.

Fig. 8. Correspondence between density of states, N(E), and number of A15 phases as functions of electron concentration. The grid of two electrons/cell is equivalent to a change of valence for the B element by one electron per atom (at 3:1 stoichiometry).

Fig. 9. Procedure for calculation of Formation Temperature Ratio (FTR) as a measure of the relative stabilities of competing solid phases. The β phase is the A15 phase.

Fig. 10. Type of reaction by which A15 phase forms upon cooling and Formation Temperature Ratio.

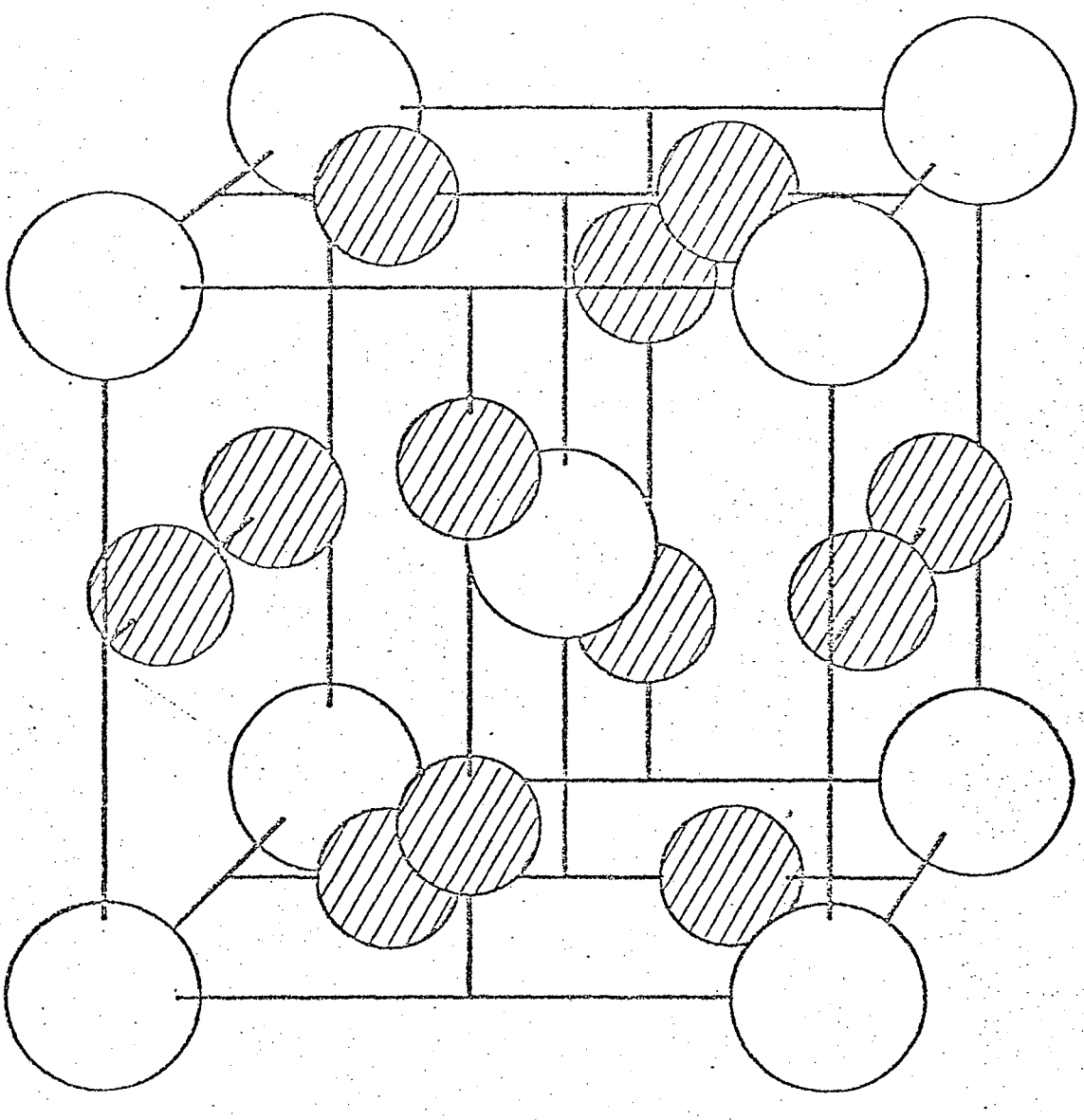

XBL 717-7039

Fig. 1

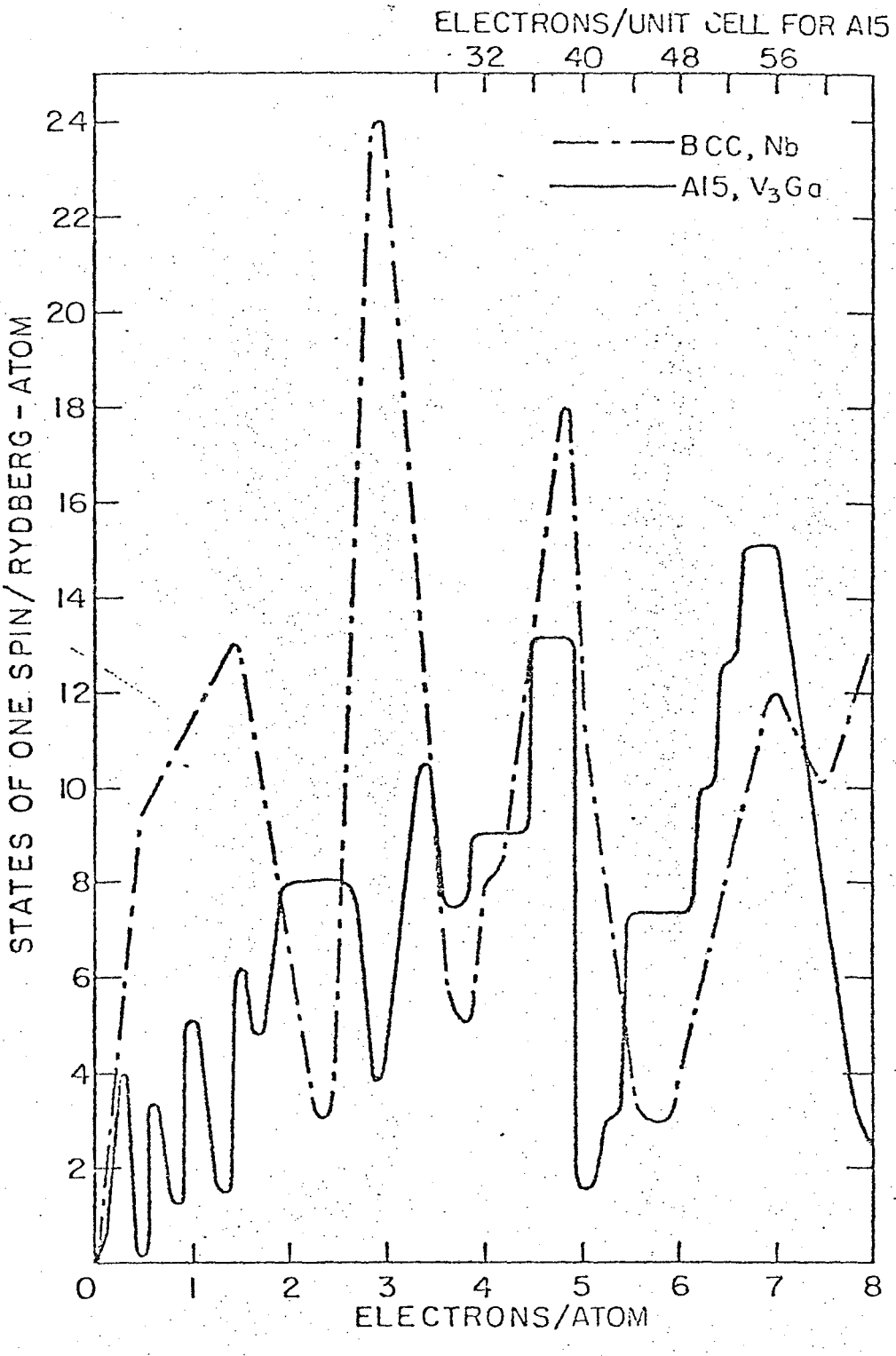

XBL 717-7046

Fig. 2

"A" ELEMENT :

TI	V	CR
ZR	NB	MO
HF	TA	W

							X			X						49			51			X	X			
																		X	X			X			
																	AL			SI		45 46	P		
							X			X						49			X	X		X	X		X	53
																		X	X			X			
MN			FE			CO			NI			CU			ZN		GA			GE	?52		AS		
					X		X	X	55	X						?49 50		?49				X		X	X
		X					X											X		X	X	X		X	
TC			RU			RH			PD			AG			CD		IN			SN	X		SB	X	
				29	X	X	X	X	X	X	X	X	X		X		48	?49			?49 50			?49	
				X	X		X	X		X	X	X	X		X		48			X	?50			X	
RE		?54	OS			IR			PT	29		AU			HG		TL			PB			BI		

Nov. 1953

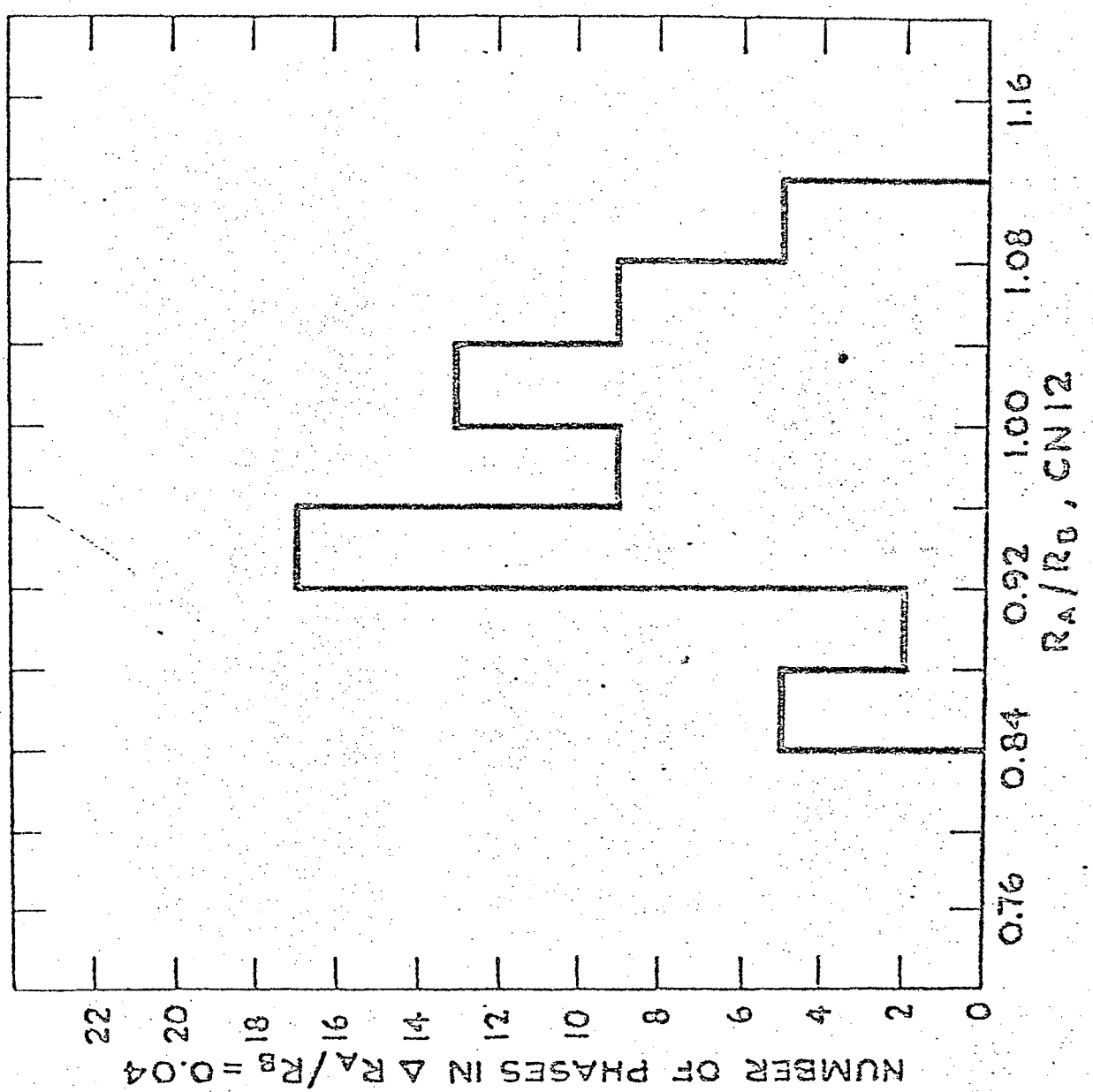
NUMBER OF PHASES IN Δ RA/Rg =0.04
0
2
4
6
8
10
12
14
16
18
20
22
0.76
0.84
0.92
1.00
1.08
1.16
RA/12b, CN12

Fig 4

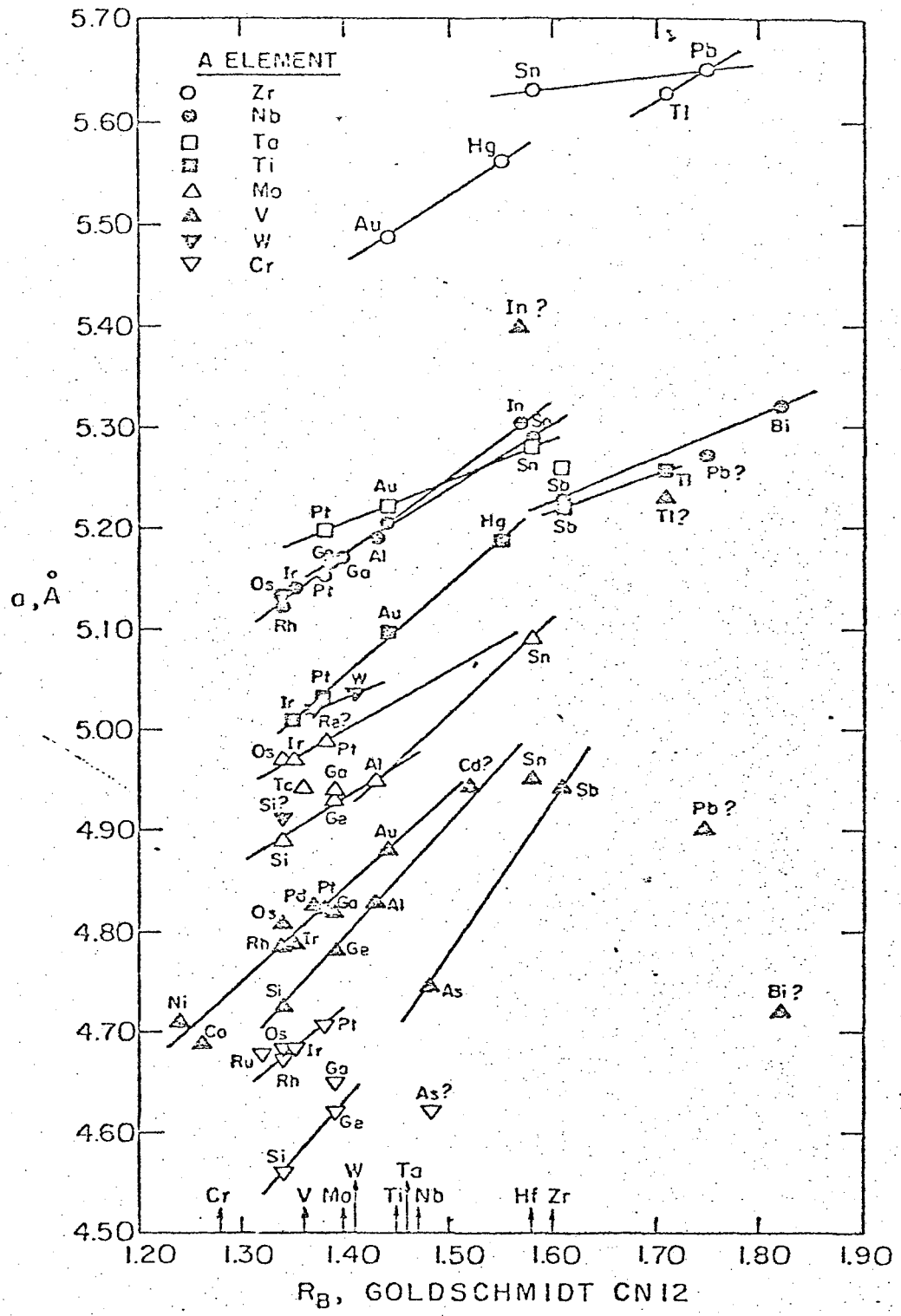

XBL717-7041

Fig. 5

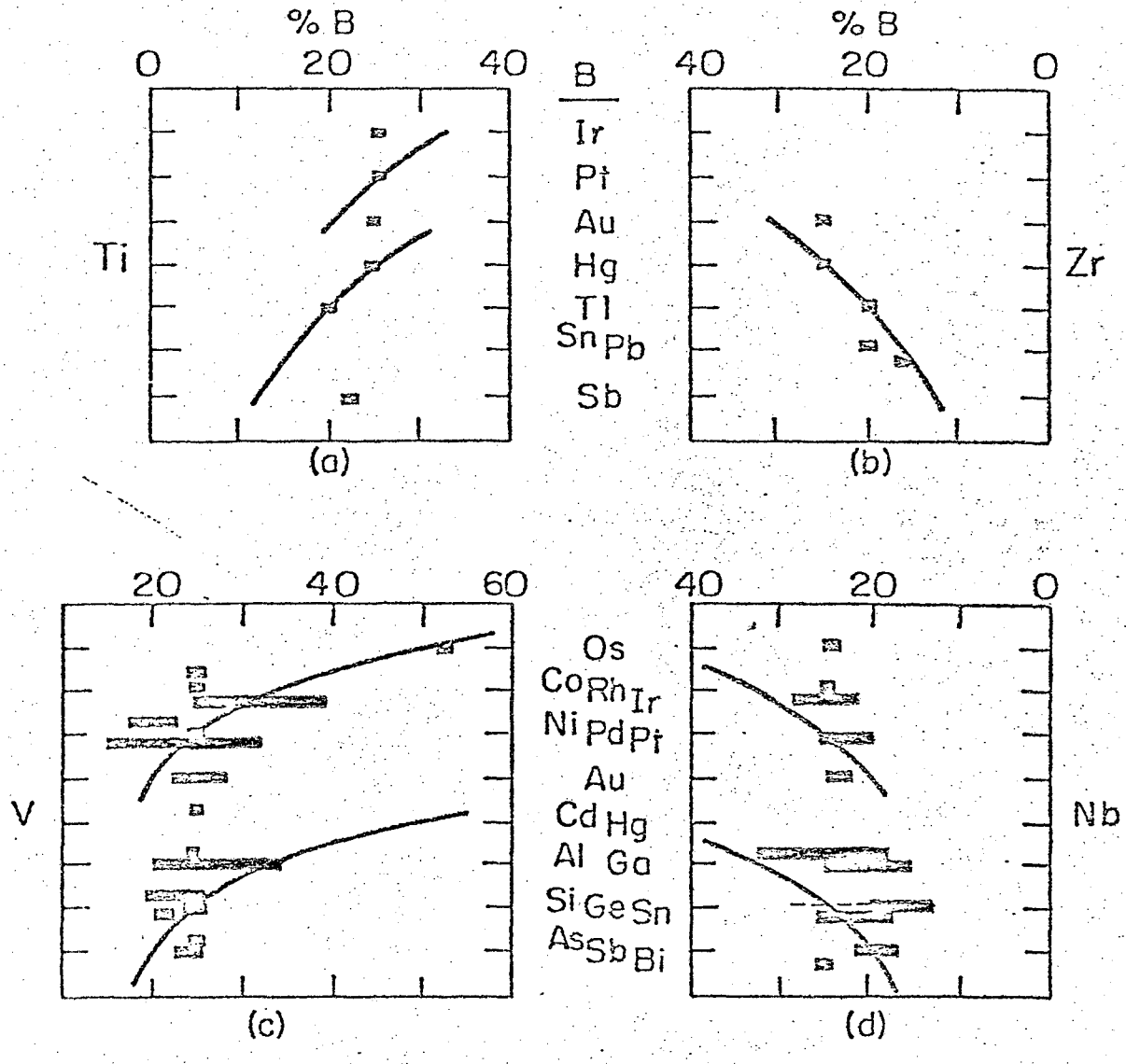

XBL 717-7042

Fig. 6

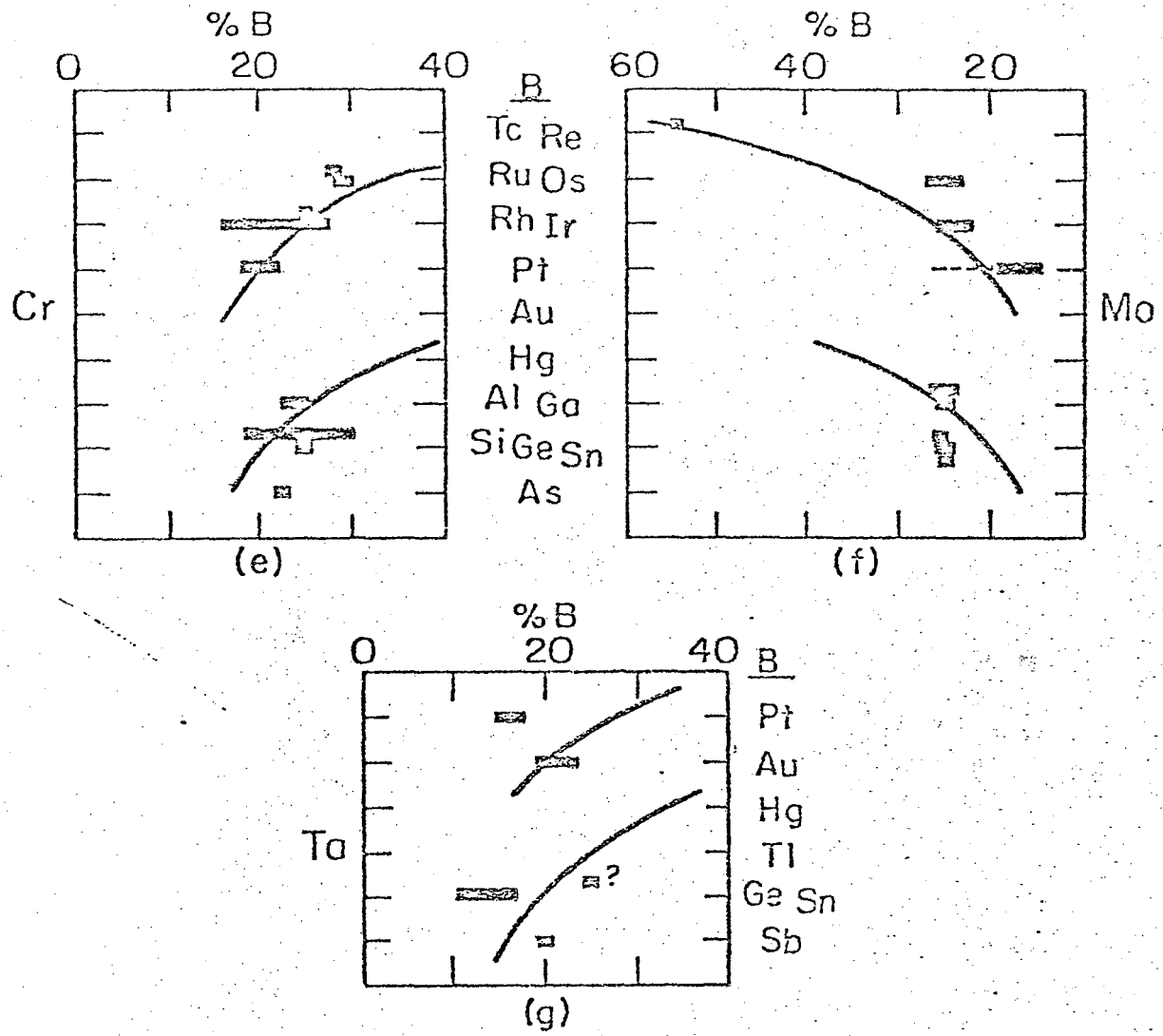

XBL717-7043

Fig 6 (cont.)

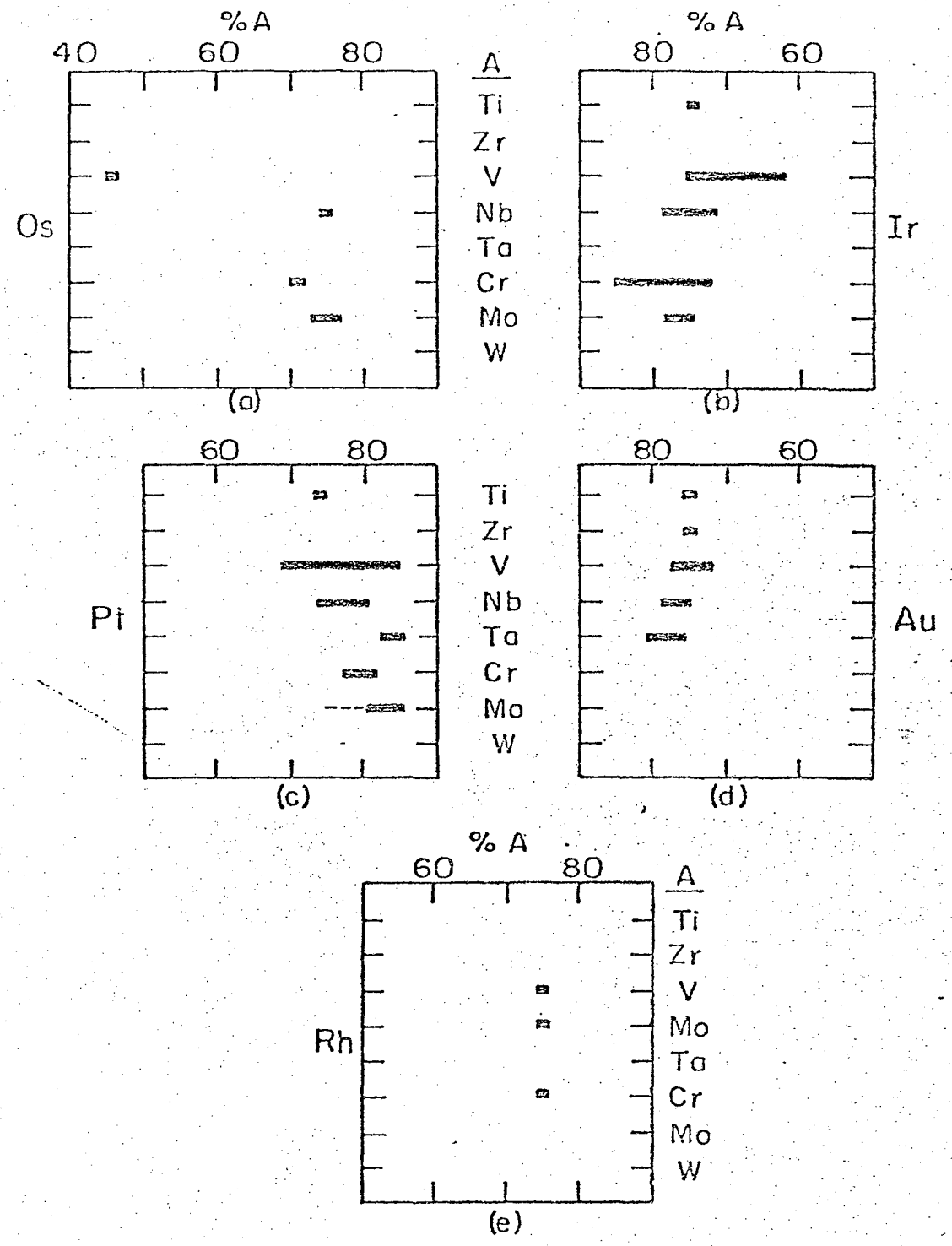

XBL 717-7044

Fig 7

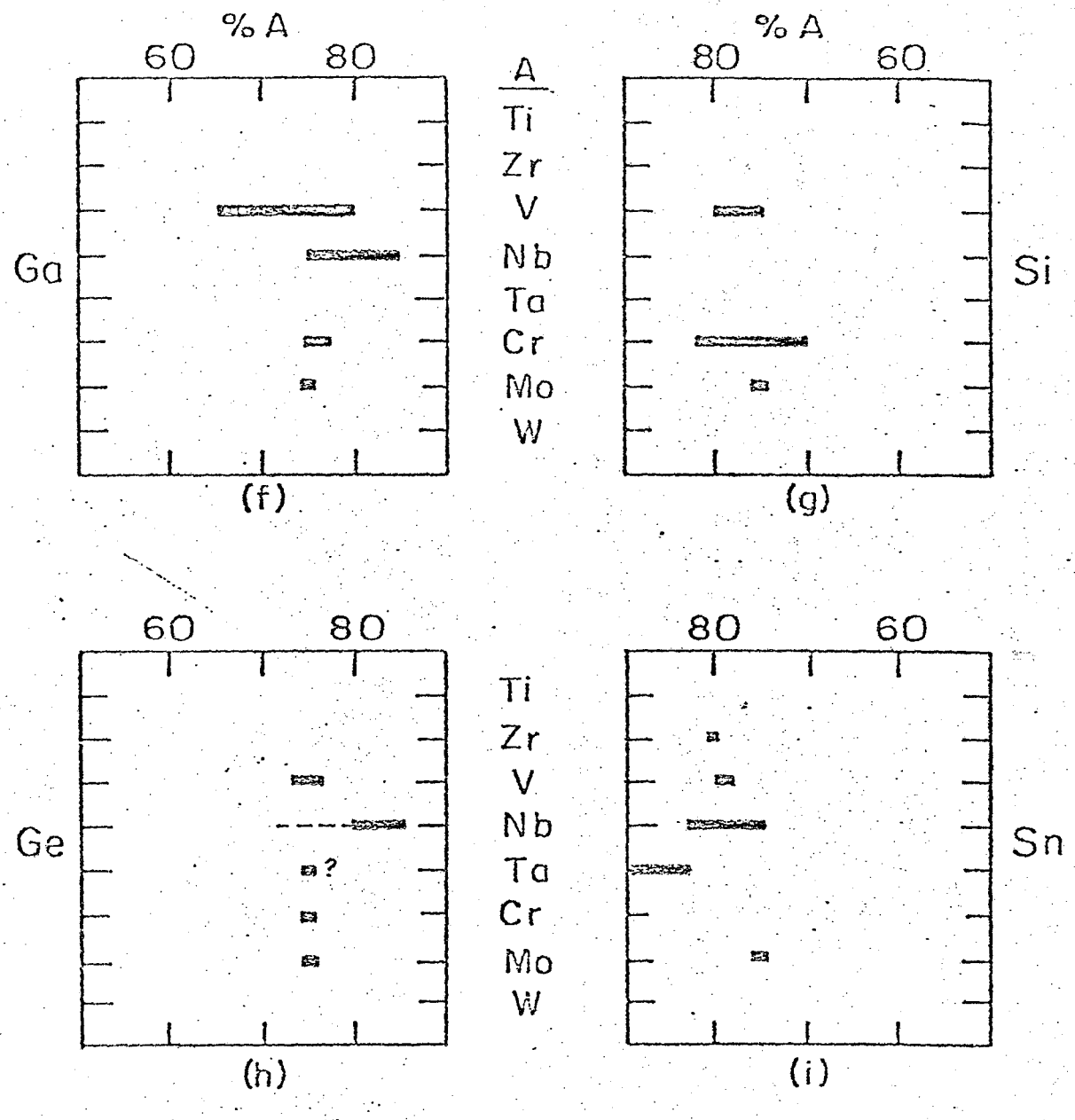

XBL717-7045

Fig. 7 (cont.)

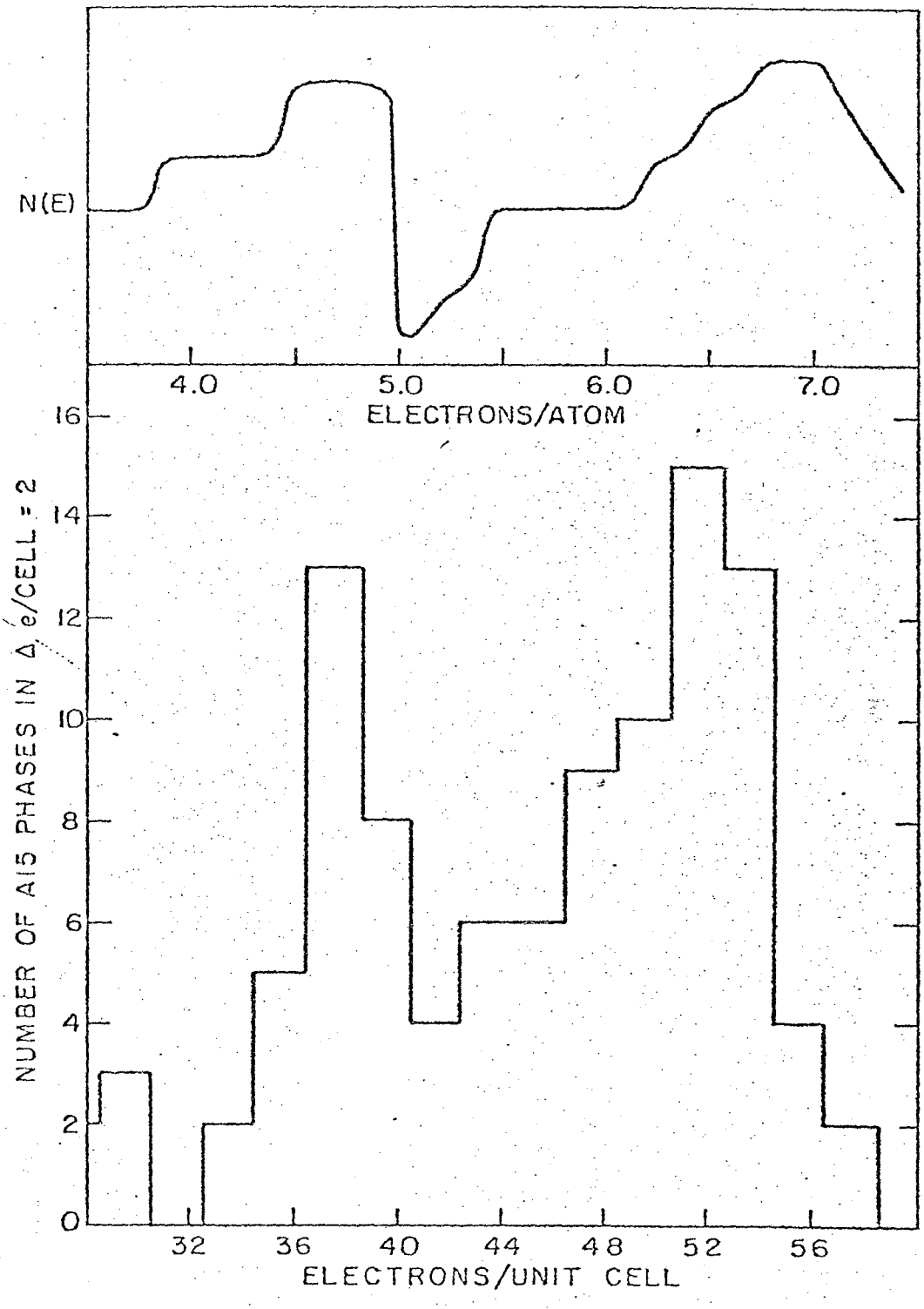

XBL717-7047

Fig 8

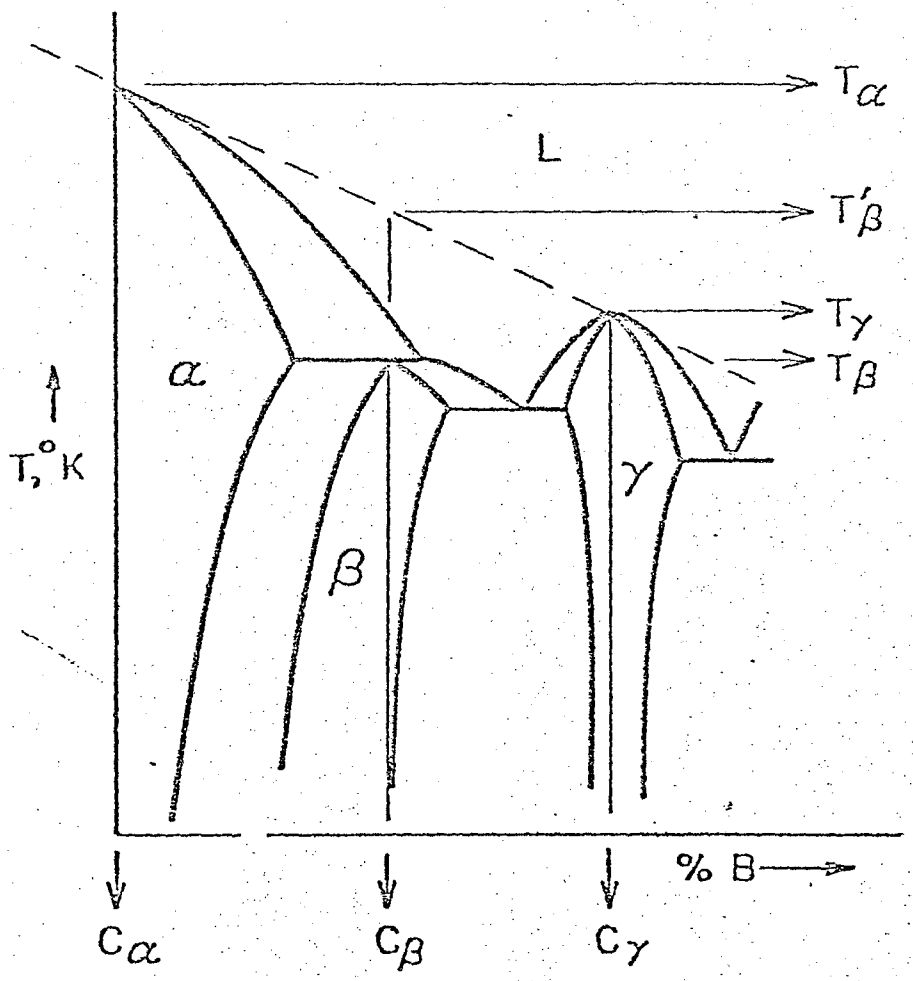

CALCULATION OF FORMATION TEMPERATURE RATIO (FTR)

$$FTR \equiv T_\beta / T'_\beta$$

$$T'_\beta = T_\alpha - (T_\alpha - T_\gamma)(C_\beta - C_\alpha)/(C_\gamma - C_\alpha)$$

XBL 717-7048

Fig 9

Type of Reaction

1 = congruent melting
2 = peritectic
3 = peritectoid
4 = congruent formation from solid
- = not enough information

"A" ELEMENT:

Ti	V	Cr
Zr	Nb	Mo
Hf	Ta	W

																						4 ~.46				2 .98	1 1.0					
																						2 .98	2 ~.90				1 .95					
																					Al				Si		3? <1.9?	P			
							3 .76			3 ~.63						-					4 .92	-			-	-			>.61		-
																						-	-			2 .89	2 .92					
Mn			Fe			Co			Ni			Cu			Zn			Ga			Ge	-		As							
					4? ~.69		-	-		3 .49						-					-			2 .90?			-	-			
		3? .89?					3 .76														-			3 .59	2 1.19	3? .25?		-			
Tc			Ru			Rh			Pd			Ag			Cd			In			Sn	2? .62?		Sb	-						
				3 -	3 .91	2 .90	-	-	1 .82	>.68	1 .81	1 .90	3 .95		4			-	-			-			-						
				3? -	3 .90		1 .99	2 .96		2 ~.97	3 <.74	3? .88?	4? -		-			-			3? .60?	-		-						
Re		3? <Br?	Os			Ir			Pt	3 .69		Au	-		Hg			Tl			Pb			Bi						

XBL 719-7248

TECHNICAL INFORMATION DIVISION
LAWRENCE BERKELEY LABORATORY
UNIVERSITY OF CALIFORNIA
BERKELEY, CALIFORNIA 94720